

Scanning transmission x-ray microscopy of isolated multiwall carbon nanotubes

A. Felten,^{a)} H. Hody, C. Bittencourt, and J.-J. Pireaux
LISE, University of Namur, 61 rue de Bruxelles, 5000 Namur, Belgium

D. Hernández Cruz and A. P. Hitchcock
Brockhouse Institute for Materials Research, McMaster University, Hamilton, Ontario L8S 4M1, Canada

(Received 8 June 2006; accepted 24 July 2006; published online 1 September 2006)

Scanning transmission x-ray microscopy (STXM) has been used to study isolated carbon nanotubes for the first time. STXM and transmission electron microscopy were applied to the same type of nanotubes, providing unique information about their composition, and electronic and structural properties. The carbon 1s near-edge x-ray absorption fine structure spectra show significant differences between multiwall carbon nanotube and carbon nanoparticle contaminants. Pristine and acid treated multiwall carbon nanotubes were also compared, highlighting the potential of the technique to differentiate surface functional groups at the nanoscale. © 2006 American Institute of Physics. [DOI: 10.1063/1.2345258]

Carbon nanotubes (CNTs) are among the most promising of advanced materials, with a wide range of potential applications including biological and chemical sensors, nanoelectronic devices, tips for scanning probe microscopy, and field emission or composite materials.^{1,2} One of the keys to achieve these goals is a precise knowledge of the properties of any given nanotube sample since the electronic properties are known to be dependent on different parameters including chirality, diameter, doping, functionalization, defects, etc.³ From this point of view, inner shell excitation by electron energy loss⁴ or by near-edge x-ray absorption fine structure (NEXAFS) spectroscopy⁵⁻⁷ is a particularly well adapted probe of carbon nanotubes. It is able to investigate both electronic and structural properties of carbon based systems, and can provide unique information about the composition of organic materials, as it can easily differentiate bonding types for carbon, oxygen, and nitrogen.⁸ However, the analysis of carbon nanotubes raises several problems, associated with their small size and often complex chemistry. Conventional spectroscopic techniques typically sample an area of some mm². Within such a large area, it is not possible to obtain reliable data on just one type of carbon nanotube. Often signal from impurities (amorphous carbon, onionlike particles, and catalysts) cannot be avoided. Furthermore, in order to remove most impurities, one has to use purification procedures that may alter the CNT structure and introduce functional groups or unwanted atoms at the CNT surface.

A way to get around these difficulties is to perform spectromicroscopy on selected zones or on isolated carbon nanotubes. In the past, this has been achieved with both scanning photoemission microscopy⁹⁻¹¹ (SPEM) and transmission electron microscope (TEM) equipped with electron energy loss spectroscopy (EELS).⁴ The spatial resolution of SPEM is at best 90 nm,⁹ which makes it a challenge to measure isolated CNT structures. While TEM-EELS does provide very high spatial resolution, two other problems exist. Much more radiation damage is produced by an electron beam relative to a photon beam¹² and the energy resolution of current TEM-EELS instruments is significantly lower than that of

synchrotron based x-ray absorption spectroscopy. It has been demonstrated that contrary to NEXAFS, TEM-EELS has failed to detect functional groups up to now.¹³

This letter reports the application of scanning transmission x-ray microscopy^{14,15} (STXM) to study the electronic and structural properties of carbon nanotubes. STXM combines both NEXAFS spectroscopy and microscopy with a spatial resolution better than 50 nm. This technique has already showed its high potential for detailed chemical nanoanalysis of polymers, biological systems, and soft materials.¹⁶ It is demonstrated that a synchrotron based spectromicroscopic technique has been able to image one isolated multiwall carbon nanotube. Furthermore, we show that STXM when combined with TEM analyses of the same location allows greatly enhanced information.

In this letter, the carbon 1s NEXAFS of multiwall carbon nanotubes (MWCNTs) is analyzed. The differences in the electronic structures of multiwall carbon nanotubes and carbon nanoparticle impurities will be shown. Then spectra of pristine and acid treated MWCNTs will be compared, underlining the unique spectroscopic features provided by STXM. The results obtained in this study open new possibilities for understanding the electronic and structural properties of carbon nanotubes.

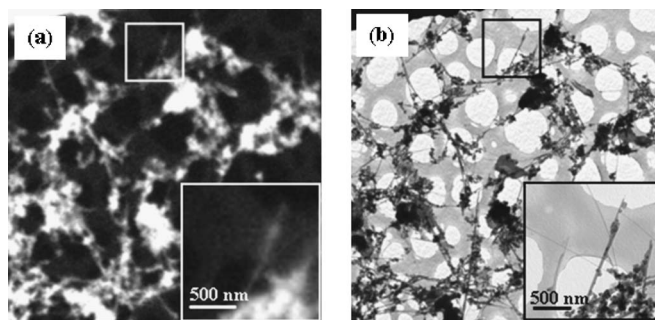


FIG. 1. (a) STXM image of a CNT powder on a holey Formvar TEM grid. The image is $10 \times 10 \mu\text{m}^2$. (b) TEM image of the same region. The inset of both images shows the region marked by a square where an isolated CNT is located.

^{a)}Electronic mail: alexandre.felten@fundp.ac.be

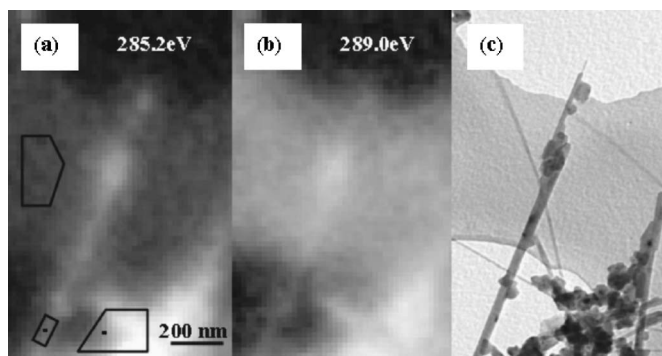


FIG. 2. STXM images at 285.2 eV (MWCNT signal enhanced) and 289.0 eV (Formvar substrate signal enhanced), and corresponding TEM picture.

Carbon nanotube powders, purchased from Mercorp (arc-discharge grown) and Nanocyl [chemical vapor deposition (CVD) grown], were sonically dispersed in ethanol and deposited on a holey Formvar TEM grid. The grid was fixed on a sample holder and inserted in the experimental chamber of the dedicated STXM (Ref. 17) on beamline 5.3.2 (Ref. 18) at the Advanced Light Synchrotron at the Lawrence Berkeley National Laboratory. The chamber is evacuated then filled with 1/3 atmosphere of helium. The monochromated x-ray beam is focused on the sample using a Fresnel zone plate. The transmitted signal is then measured with single photon counting using a phosphor converter and a high performance photomultiplier tube. The energy resolution of the beamline is 150 meV and the spatial resolution is 40 nm with the zone plates used (35 nm outer zones).

Figure 1(a) shows a STXM image of a region of the grid covered with Mercorp carbon nanotube powder and collected at 285.2 eV which is the energy of the $1s \rightarrow \pi^*$ transition in sp^2 hybridized C atoms. The very same region has been imaged using an 80 keV transmission electron microscope in Fig. 1(b). It can be seen from these two images that the nanotube powder contains a lot of agglomerated bundles and impurities. However, individual multiwall carbon nanotubes are also present with a few lying on top of holes in the Formvar coating on the TEM grid. A closer look to this region reveals that an isolated multiwall carbon nanotube can be seen. TEM preanalysis is very useful and time saving since it allows identification of good regions for STXM measurements which contain isolated carbon nanotubes.

STXM can be used in different modes (point, line scan spectrum, or image sequence mode) but gives the most detailed information when it is used to acquire a sequence of images over a range of photon energies (also called a stack). This information is equivalent to obtaining a complete NEXAFS spectrum at each pixel. Such sequences can be processed to derive a quantitative chemical map of the analyzed region by fitting the spectrum of each pixel to a set of suitable reference spectra and thus providing compositional information at the scale of individual pixels. Figure 2 shows 2 of 60 STXM images acquired between 282 and 310 eV on the nanotube displayed in the inset of Fig. 1. A pixel size of 20 nm and a dwell time (counting period at each pixel) of 5 ms were used. The energy step was 0.2 eV from 284 to 290.2 eV and 0.6 eV from 290.8 to 300 eV. The image at 285.2 eV enhances the signal of the nanotube powder while that at 289 eV enhances the Formvar substrate. The diameter of the multiwall carbon nanotube measured from the TEM image [Fig. 2(c)] is 40 nm.

Three regions are highlighted in Fig. 2(a) and by comparison with the TEM image, they can be attributed without doubt to the Formvar substrate, an isolated multiwall carbon nanotube, and material containing both carbon nanoparticles (CNPs) and nanotubes. The corresponding NEXAFS spectra of these three regions are compared in Fig. 3(a) while Fig. 3(b) plots the spectra of a single pixel on the carbon nanotube and a single pixel on the carbon nanoparticle. The C $1s$ spectrum of the MWCNT is very similar to that of highly oriented pyrolytic graphite^{6,19} and is characterized by a sharp peak at 285.2 eV which corresponds to the $1s \rightarrow \pi^*$ transition in sp^2 hybridized C atoms and by a broader peak at 291.5 eV which is the $1s \rightarrow \sigma^*$ resonance. This similarity of the NEXAFS spectra of nanotubes and graphite indicates that the MWCNT has the structure of rolled graphene sheets with very few defects which is characteristic of arc-discharge grown nanotubes. High resolution TEM analyses were performed on the same type of MWCNTs and confirmed the high quality of their structure. The spectra of CNP+CNT region in Fig. 3(a) and of the CNP in Fig. 3(b) exhibit the same features at 285.2 and 292 eV but there are also some differences. In particular, the $1s \rightarrow \pi^*$ peak has reduced intensity relative to that for the carbon nanotube, which indicates that the particles contain less sp^2 hybridized carbon compared to carbon nanotubes. Confirmation can be found in the $1s \rightarrow \sigma^*$ transition which has a smoother edge in the

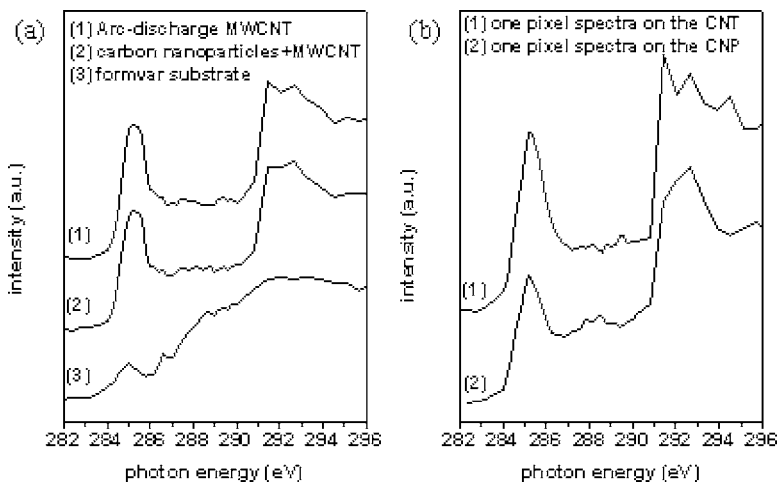


FIG. 3. (a) Spectra of arc-discharge MWCNT, MWCNT+CNP powder, and Formvar substrate. (b) One pixel spectra taken on the MWCNT and on the CNP.

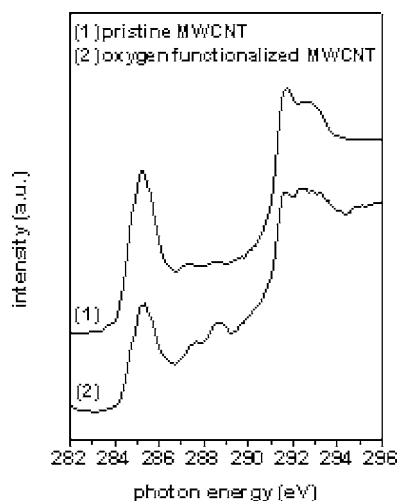


FIG. 4. Spectra of (1) pristine and (2) acid treated CVD MWCNTs.

nanoparticle spectrum, characteristic of a disordered sp^2 matrix and the presence of an sp^3 phase.²⁰ Furthermore, the region between 287 and 290 eV presents a weak maximum in the case of the nanoparticles which is attributed to hydrogenated carbon^{13,21} included in the particles, as well as a small amount of adsorbed oxygen.¹⁹

Modification of surface properties of carbon nanotubes is an important issue for a number of applications. The ability of STXM to differentiate surface functional groups is demonstrated by comparing pristine and acid treated Nanocyl MWCNTs. Line scan spectra were acquired in selected regions by recording the same line on the sample at successive photon energies such that a NEXAFS spectrum is acquired at each point on the line. The energy step was 0.1 eV and the dwell time per pixel was 10 ms. Spectra of both types of nanotubes are shown in Fig. 4. The C 1s NEXAFS of the pristine CNT is characterized by features at 285.2, 291.7, and 292.8 eV which are characteristic of sp^2 carbon. Some other small features can be observed between 287 and 290 eV, indicating the presence of CH_x bonds or adsorption of residual oxygen at the surface.¹⁸ After acid treatment, two nicely resolved peaks appear at 287.5 and 288.6 eV. These peak can be attributed to oxygen containing groups and correspond, respectively, to C=O and COOH.^{13,22}

In conclusion, the results obtained show that STXM can provide C 1s NEXAFS spectra of isolated MWCNTs. This circumvents the sampling ambiguity inherent in nonspatial resolved NEXAFS methods while keeping the advantages of high energy resolution and low radiation damage of x-ray excited inner shell spectroscopy. This approach opens new possibilities for fundamental and applied studies of the electronic and structural properties of carbon nanotubes. One could imagine for instance comparing nanotubes of different diameters or growth methods, studying grafting of functional groups on the nanotube surface, comparing the electronic properties of the tips and body of a nanotube, or to look for contact properties with metals.

This work was supported by the Région Wallone (Belgium), PAI5/1/1 on “Quantum Size Effects in Nanostruc-

tured Materials” (Belgium), the Nanobeams EU Network of Excellence, NSERC (Canada), and the Canada Research Chair program (APH). Construction and operation of the STXM5.3.2 microscope is supported by NSF DMR-9975694, DOE DE-FG02-98ER45737, Dow Chemical, NSERC, and the Canada Foundation for Innovation. Zone plates were supplied by the Centre for X-ray Optics, LBNL. The authors thank A. L. D. Kilcoyne and T. Tyliczszak for their expert work in developing and maintaining STXM532. The Advanced Light Source is supported by the Director, Office of Energy Research, Office of Basic Energy Sciences, Materials Sciences Division of the U.S. Department of Energy, under Contract No. DE-AC03-76SF00098.

¹J. Robertson, *Mater. Today* **7**, 46 (2004).

²R. H. Baughman, A. A. Zakhidov, and W. A. de Heer, *Science* **297**, 787 (2002).

³H. Dai, *Surf. Sci.* **500**, 218 (2002).

⁴O. Stephan, M. Kociack, L. Henrard, K. Suenaga, A. Gloter, M. Tence, E. Sandre, and C. Colliex, *J. Electron Spectrosc. Relat. Phenom.* **209**, 114 (2001).

⁵J. Zhong, L. Song, Z.-Y. Wu, S.-S. Xie, M. Abbas, K. Ibrahim, and H. Qian, *Carbon* **44**, 866 (2006).

⁶Y. H. Tang, T. K. Sham, Y. F. Hu, C. S. Lee, and S. T. Lee, *Chem. Phys. Lett.* **366**, 636 (2002).

⁷S. Banerjee, T. Hemraj-Benny, S. Sambasivan, D. A. Fischer, J. A. Misewich, and S. Wong, *J. Phys. Chem. B* **109**, 8489 (2005).

⁸B. Watta, L. Thomsen, and P. C. Dastoor, *J. Electron Spectrosc. Relat. Phenom.* **151**, 105 (2006).

⁹A. Goldoni, R. Larciprete, L. Gregoratti, B. Kaulich, M. Kiskinova, Y. Zhang, H. Dai, L. Sangaletti, and F. Parmigiani, *Appl. Phys. Lett.* **80**, 2165 (2002).

¹⁰S. Suzuki, Y. Watanabe, T. Ogino, Y. Homma, D. Takagi, S. Heun, L. Gregoratti, A. Barinov, and M. Kiskinova, *Carbon* **42**, 559 (2004).

¹¹J. W. Chiou, C. L. Yueh, J. C. Jan, H. M. Tsai, W. F. Pong, I.-H. Hong, R. Klausner, M.-H. Tsai, Y. K. Chang, Y. Y. Chen, C. T. Wu, K. H. Chen, S. L. Wei, C. Y. Wen, L. C. Chen, and T. J. Chuang, *Appl. Phys. Lett.* **81**, 4189 (2002).

¹²E. G. Rightor, A. P. Hitchcock, H. Ade, R. D. Leapman, S. G. Urquhart, A. P. Smith, G. Mitchell, D. Fischer, H. J. Shin, and T. Warwick, *J. Phys. Chem. B* **101**, 1950 (1997).

¹³A. Braun, F. E. Huggins, N. Shah, Y. Chen, S. Wirick, S. B. Mun, C. Jacobsen, and G. P. Huffman, *Carbon* **43**, 117 (2005).

¹⁴H. Ade, in *Experimental Methods in the Physical Sciences*, edited by J. A. R. Samson and D. L. Ederer (Academic, New York, 1998), Vol. 32, p. 225.

¹⁵H. Ade and S. G. Urquhart, in *Chemical Applications of Synchrotron Radiation*, edited by T. K. Sham (World Scientific, Singapore, 2002), 12A, pp. 285–335.

¹⁶A. P. Hitchcock, H. D. H. Stover, L. M. Croll, and R. F. Childs, *Aust. J. Chem.* **58**, 423 (2005).

¹⁷A. L. D. Kilcoyne, T. Tyliczszak, W. F. Steele, S. Fakra, P. Hitchcock, K. Franck, E. Anderson, B. Harteneck, E. G. Rightor, G. E. Mitchell, A. P. Hitchcock, L. Yang, T. Warwick, and H. Ade, *J. Synchrotron Radiat.* **10**, 125 (2003).

¹⁸T. Warwick, H. Ade, A. L. D. Kilcoyne, M. Kritscher, T. Tyliczszak, S. Fakra, A. P. Hitchcock, P. Hitchcock, and H. A. Padmore, *J. Synchrotron Radiat.* **9**, 254 (2002).

¹⁹M. Abbas, Z. Y. Wu, J. Zhong, K. Ibrahim, A. Fiori, S. Orlanducci, V. Sessa, M. L. Terranova, and I. Davoli, *Appl. Phys. Lett.* **87**, 051923 (2005).

²⁰R. Larciprete, S. Lizzit, S. Botti, C. Cepek, and A. Goldoni, *Phys. Rev. B* **66**, 121402 (2002).

²¹A. Nikitin, H. Ogasawara, D. Mann, R. Denecke, Z. Zhang, H. Dai, K. J. Cho, and A. Nilsson, *Phys. Rev. Lett.* **95**, 225507 (2005).

²²A. Kuznetsova, I. Popova, J. T. Yates, M. J. Bronikowski, C. B. Huffman, J. Liu, R. E. Smalley, H. H. Hwu, and J. G. Chen, *J. Am. Chem. Soc.* **123**, 10699 (2001).